

Structure of the electrical double layer on Ag(100): Promotive effect of cationic species on Br adlayer formation

Masashi Nakamura (中村 将志),^{1,*} Yo Nakajima (中島 陽),¹ Narumasa Sato (佐藤 成真),¹
Nagahiro Hoshi (星 永宏),¹ and Osami Sakata (坂田 修身)²

¹Department of Applied Chemistry and Biotechnology, Graduate School of Engineering, Chiba University, Yayoi-cho 1-33,
Inage-ku, Chiba 263-8522, Japan

²Synchrotron X-ray Station at Spring-8, National Institute for Materials Science (NIMS), Kouto 1-1-1, Sayo-gun, Hyogo 679-5148, Japan.

(Received 19 September 2011; published 20 October 2011)

We revealed the promotive effect of alkali metal cations on Br adlayer formation on an Ag(100) electrode by *in-situ* measurement of the x-ray specular rod. Alkali metal cations in the electrical double layer affect the onset potential of Br adsorption and the order-disorder transition. We determined the Cs structure in the electrical double layer during Br adlayer formation and found that (1) the Cs structure depends on the coverage of adsorbed Br, and (2) the amount of Cs increases at the initial stage of Br adlayer formation. Structural analysis suggests that hydrated Cs is localized in the area around adsorbed Br via noncovalent interactions. Formation of a Cs-Br complex promotes Br adsorption.

DOI: [10.1103/PhysRevB.84.165433](https://doi.org/10.1103/PhysRevB.84.165433)

PACS number(s): 68.08.-p, 68.35.Rh, 73.30.+y, 82.45.-h

I. INTRODUCTION

The electrical double layer (EDL) at the solid-liquid interface is an important research topic because EDL structure and composition govern electrochemical processes. Ionic adsorption-desorption and the order-disorder transition of the adlayer are important steps in many electrochemical reactions. The specifically adsorbed ionic layer, called the inner Helmholtz plane (IHP), has been widely studied using various surface science techniques.^{1,2}

In contrast, there has been little structural research for the outer Helmholtz plane (OHP) and the diffuse layer above the IHP, owing to the limitations of *in-situ* analytical methods. OHP species also play an essential role for electrochemical reactions. Cyclic voltammograms (CVs) in different alkali metal (AM) ion solutions show that these steps depend on the cationic species.^{3,4} Nonspecifically adsorbed cations are known to affect the catalytic activity of fuel cell reactions through noncovalent interaction.^{5,6} Noncovalent interactions between adsorbed and nonadsorbed species often result in a structural gap between electrochemical and ultrahigh vacuum (UHV) conditions.^{7,8} Thus, weak interactions, such as hydrogen bonding and electrostatic forces, affect adsorbed layer stability and electrochemical reactions significantly. However, the structure and nature of charged species above the IHP have been longstanding issues in interface science.

The order-disorder transition in the ionic adsorption layer has been widely studied by experimental methods and theoretical simulations using a lattice-gas model.^{1,9} Br on Ag(100) is a good prototype to study the two-dimensional order-disorder transition.¹⁰⁻¹⁷ Below the order-disorder transition potential, Br is adsorbed in a disordered fashion onto the fourfold hollow site of Ag(100). Above the order-disorder transition potentials, Br completely occupies at the $c(2 \times 2)$ sublattice. Br adlayer formation on Ag(100) has been explained by the Ising model, assuming nearest neighbor repulsion and long-range Coulomb repulsion between adsorbed Br (Br_{ad}).^{10,11} Monte Carlo simulation using the Ising Hamiltonian suggests that surface water and OHP cations are not necessary for the reproduction of the characteristic peaks of the CV.¹¹⁻¹⁴ Br

adsorption in the disordered region is dominated by the interatomic interaction of Br_{ad} . However, CV of Ag(100) in CsBr differs from that in LiBr remarkably, as shown in Fig. 1. This finding suggests that the cationic species above the IHP interact with the specifically adsorbed Br, which affects the adlayer formation and the order-disorder transition.

Full structural analysis of the EDL is essential for understanding the nature of adsorption-desorption and order-disorder transition. The recent surface x-ray diffraction (SXD) study has successfully determined the detailed OHP structure of hydrated Cs above an ordered $c(2 \times 2)$ -2Br adlayer on Ag(100).⁴ X-ray diffraction can reveal the structure of both the adsorbed and nonadsorbed species in the EDL.^{4,18,19} In this paper, the Cs structure on Ag(100) during Br adlayer formation was investigated using *in-situ* measurement of the x-ray specular rod. We report the structural effects of Cs on the Br adsorption and the order-disorder transition.

II. EXPERIMENTS

An Ag(100) crystal surface (Surface Preparation Laboratory) was etched in chromic acid solution, and then annealed in $\text{H}_2 + \text{Ar}$ using an induction heating furnace (AMBRELL) for the preparation of an atomically flat surface. The pHs of CsBr, KBr, and LiBr (Aldrich) solution were adjusted to 12.5 using CsOH, KOH, and LiOH (Aldrich), respectively, in order to inhibit the hydrogen evolution reaction at the negative potentials. The concentration of Cs^+ was adjusted with CsF (Aldrich). All electrode potentials were referred to Ag/AgCl. X-ray measurements were performed with a multi-axis diffractometer at the BL13XU, Spring-8, Japan²⁰ at an x-ray beam energy of 12.4 keV. Integrated intensities were measured by rocking scans then corrected for sample area, Lorentz factor, and polarization factor. A body-centered tetragonal (bct) coordinate system was used to describe the reciprocal vector as $Q = Ha^* + Kb^* + Lc^*$, where $a^* = b^* = 2\pi/a$, $c^* = \sqrt{2}\pi/a$, $a = 2.889 \text{ \AA}$, and L is the direction normal to the surface. Structure refinements were performed using the least-squares method with the ANA-ROD program.²¹

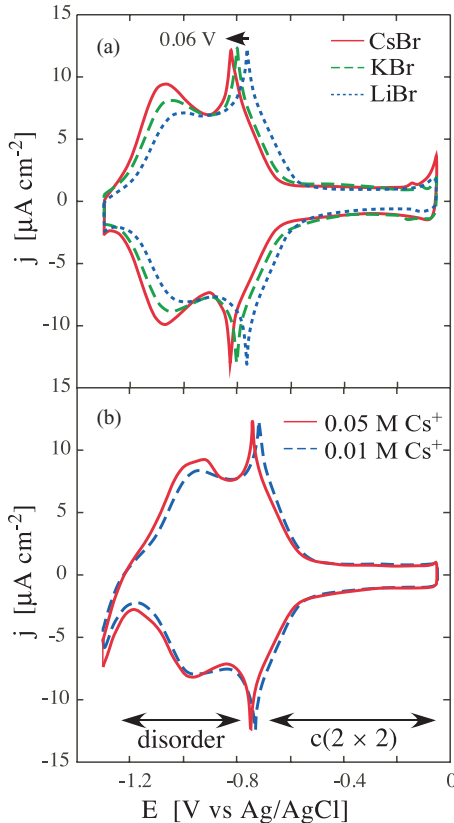


FIG. 1. (Color online) (a) Cyclic voltammograms of Ag(100) in 0.1 M CsBr + 0.05 M CsOH (solid line), 0.1 M KBr + 0.05 M KOH (dashed line), and 0.1 M LiBr + 0.05 M LiOH (dotted line). (b) Cyclic voltammograms of Ag(100) in different Cs⁺ concentration: 0.01 M CsBr + 0.04 M CsF (solid line) and 0.01 M CsBr (dashed line). The scanning rate is 0.05 V s⁻¹.

The detailed procedure for the structural analysis is given in previous reports.^{4,18}

III. RESULTS AND DISCUSSION

Figure 1 shows CVs of Ag(100) in AMBr (AM = Cs, K, and Li). The pair peaks around -0.8 V and the broad peaks at -1.1 V have been assigned to the order-disorder transition and the adsorption-desorption of Br_{ad}, respectively.¹⁰ The voltammetric features of Br adsorption on Ag(100) clearly depend on the AM counter cations. Counter cations cause the peak potential of the order-disorder transition around -0.8 V to shift and the prewave around -1.1 V to increase gradually in the order Cs > K > Li [Fig. 1(a)]. Concentration dependence of Cs⁺ in CsBr shows similar results as shown in Fig. 1(b). Since the concentration of Br⁻ is constant, these results suggest that heavy cations, such as Cs and K, strongly affect Br adlayer formation. For the elucidation of the effect of cationic species, we measured the specular 00 rod of Ag(100) in the potential range from the Br adsorption to the ordered $c(2 \times 2)$ -2Br formation. Our previous result for the $c(2 \times 2)$ -2Br layer on Ag(100) shows that the specular rod in CsBr differs from that in LiBr above -0.6 V significantly.⁴ Localization of the heavy atom (Cs) in the EDL causes a typical change in the rod profile. However, at -1.3 V, the profile in CsBr becomes very

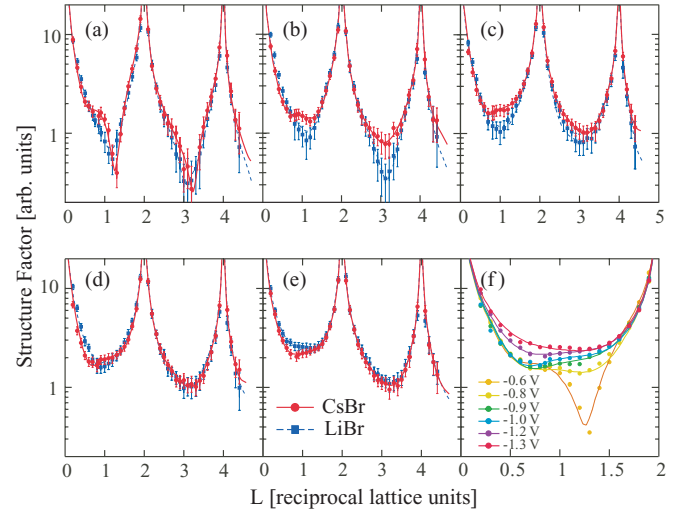


FIG. 2. (Color) Specular rod profiles of Ag(100) in 0.1 M CsBr + 0.05 M CsOH (circle) and 0.1 M LiBr + 0.05 M LiOH (square) at various potentials vs Ag/AgCl (a) -0.6 , (b) -0.8 , (c) -0.9 , (d) -1.0 , and (e) -1.2 V. (f) Potential dependence of the specular rod in CsBr at lower L. Solid and dashed lines are structure factors calculated from optimized models.

similar to that in LiBr, indicating that the vertically ordered structure of Cs disappears at -1.3 V. Detailed structural analysis reveals that neither Br nor Cs are layered in the EDL. Above -1.25 V, anodic and cathodic current due to the Br adsorption-desorption is associated with counter cations. X-ray diffraction cannot determine the charge of ionic species. In the case of Cs on $c(2 \times 2)$ -2Br, we report that OHP-Cs moves away from the surface at positive potentials.⁴ This result indicates that OHP-Cs has a positive charge.

Figure 2 shows the specular rod profiles on Ag(100) between -1.2 and -0.6 V in LiBr and CsBr. The rod profiles in CsBr are different from those in LiBr significantly [Figs. 2(a)–2(e)]. The specular rods depend on the applied potential strongly in CsBr, as shown in Fig. 2(f). The profiles in LiBr are smooth in shape. In CsBr, however, the asymmetry at the dip and the bulge between the Bragg peaks are observed because of the layered structure of Cs in the EDL. These results are similar to those above -0.6 V.⁴ Cs is localized in the EDL during the formation of the Br adlayer. Li cations will also be localized in the electrical double layer. However, the contribution of Li layer to the scattered x ray is extremely weak, because the scattering cross section of Li is significantly smaller than that of Cs.

We performed structural analyses by the optimization of the occupancies, the vertical positions, and Debye–Waller factors. The model was composed of Br_{ad}, Cs, and the substrate Ag for the first and the second Ag layers.⁴ Although we considered buckling of the second Ag layer, we could not distinguish atomic fluctuations in the second layer. The buckling causes oscillation in fractional order rods, but the small fluctuations of the inner layer do not influence the crystal truncation rods and the specular rod significantly.^{4,22–24}

Table I lists the vertical layer spacing and the coverage of the optimized model in LiBr and CsBr at the potentials below -0.6 V. The layer spacing and the coverage are plotted against

TABLE I. Vertical layer spacing (\AA) and the coverage (ML) for the optimized model in LiBr and CsBr.

	Electrode Potential E [V vs Ag/AgCl]				
	-1.2	-1.0	-0.9	-0.8	-0.6
$d_{\text{Ag-Br}}$ (LiBr)	1.80 ± 0.25	1.80 ± 0.06 (1.80 ± 0.18)	1.85 ± 0.04 (1.85 ± 0.06)	1.89 ± 0.04 (1.95 ± 0.05)	1.97 ± 0.03 (1.93 ± 0.04)
$d_{\text{Cs-Br}}$	1.45 ± 0.36	1.72 ± 0.21	1.67 ± 0.14	2.03 ± 0.15	2.67 ± 0.11
θ_{Br} (LiBr)	0.051 ± 0.026 (0)	0.228 ± 0.027 (0.081 ± 0.032)	0.263 ± 0.024 (0.222 ± 0.035)	0.329 ± 0.024 (0.310 ± 0.034)	0.485 ± 0.032 (0.419 ± 0.032)
θ_{Cs}	0.057 ± 0.018	0.126 ± 0.024	0.102 ± 0.019	0.084 ± 0.024	0.128 ± 0.021

the applied potentials in Fig. 3. The Ag-Br layer spacing expands slightly from $1.80 \pm 0.25 \text{ \AA}$ (-1.2 V) to $1.97 \pm 0.03 \text{ \AA}$ (-0.6 V). On the strongly corrugated Ag(100) surface, the preferential adsorption site of Br is the fourfold hollow site. Density functional theory (DFT) calculations suggested that the hollow site is more stable than the bridge and the top sites by 0.21 and 0.56 eV, respectively.¹⁶ Therefore, the variation of

the Ag-Br layer spacing is not due to the site conversion, but rather due to the relaxation of the Ag-Br bond with the increase in Br coverage. Similar layer spacing dependence was reported for Cl adsorbed on Cu(100) as determined by SXD.²⁴ Potential dependence of the Ag-Br layer spacing is similar to those in LiBr and in CsBr.

For the Br coverage in LiBr [Fig. 3(b)], the plot corresponds to the simulation result [solid and dashed lines in Fig. 3(b)] of the adsorption isotherm using quasichemical approximation reported previously.¹¹ Br coverage linearly increases with increasing potential and reaches saturation coverage of $\theta_{\text{Br}} = 0.5$ at -0.4 V , at which the $c(2 \times 2)$ structure is completed. In contrast, in CsBr, the potential dependence of Br coverage deviates from the simulated isotherm at the initial stage of Br adsorption ($< -1.0 \text{ V}$). Br adlayer formation in CsBr cannot be explained by the simple lattice-gas model that assumes nearest neighbor repulsion and long-range Coulomb repulsion between adsorbed Br_{ad} . Thus, the presence of Cs promotes Br adsorption at low Br coverage significantly.

Specular rod analysis shows the existence of Cs in the EDL above -1.2 V as shown in Fig. 3(b). In a previous study on the $c(2 \times 2)$ region, we reported that hydrated Cs is located at the hollow site of the $c(2 \times 2)$ -2Br, and the amount of the OHP-Cs decreases at positive potentials because of repulsive interaction with the surface charge.⁴ However, Cs coverage increases with increasing potential below -1.0 V , which suggests that attractive interaction of Cs with Br_{ad} overwhelms the electrostatic repulsion. The distance of the Cs layer from the surface increases with increasing potential [Fig. 3(a)].

At the potential region below -0.8 V , the in-plane structures of Cs and Br cannot be determined by SXD because of the disordered structures. We infer the schematic models and the interaction of Cs and Br on the basis of the vertical information and the coverage obtained from specular rod analysis. At -1.3 V , Cs and Br are not adsorbed on Ag(100). At -1.2 V , however, they have a double-layered structure with the same coverage. The layered structure of Cs is caused by the interaction with Br_{ad} at the initial stage of Br adsorption. The Ag-Cs layer spacing is $3.25 \pm 0.61 \text{ \AA}$ at -1.2 V , which corresponds to that of directly adsorbed Cs on Ru(001) as determined by the low-energy electron diffraction (LEED).²⁵ However, the distance of Cs from the surface increases with a slope similar to that for the $c(2 \times 2)$ -2Br above -0.6 V [Fig. 3(a)]. This behavior indicates that Cs is noncovalently interacted with the surface and Br_{ad} via hydration water. We previously reported a similar hydration structure on the

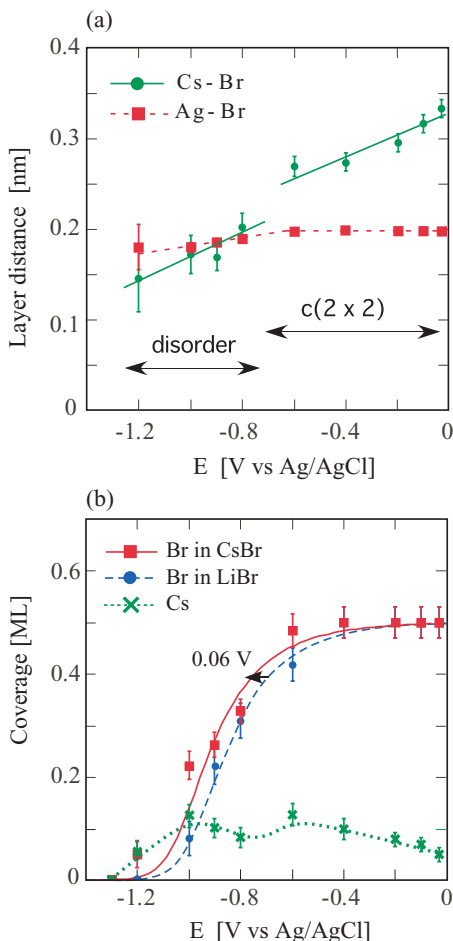


FIG. 3. (Color online) (a) Potential dependence of the layer spacing and (b) the coverage in LiBr and CsBr. Data above -0.4 V and at -1.3 V are from Ref. 4. The dashed line in (b) is fit to a Br isotherm using the quasichemical approximation (Ref. 11). The solid line in (b) is shifted by -0.06 V from the dashed line, which corresponds to the peak shift of the order-disorder transition observed in Fig. 1(a).

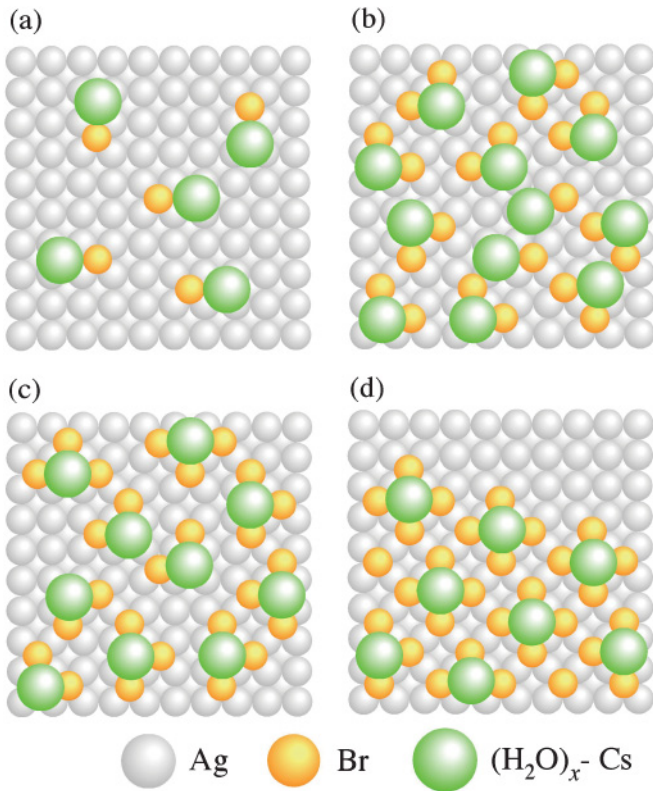


FIG. 4. (Color online) Schematic models of Br and Cs on Ag(100) on the basis of the vertical information and the coverage at various potentials: (a) -1.2 , (b) -1.0 , (c) -0.9 , and (d) -0.8 V (Ag/AgCl).

$c(2 \times 2)$ -2Br as determined by the DFT calculations: a single layer of water is intercalated between the OHP-Cs and the IHP- Br_{ad} .⁴ Adsorption models of Br_{ad} and Cs on Ag(100) are schematically shown in Fig. 4 on the basis of the vertical information and the coverage. Although there is no structural information of the in-plane structure, Cs will be arranged around adsorbed Br_{ad} at the hollow site through noncovalent interaction [Fig. 4(a)]. Formation of the Cs-Br complex promotes Br adsorption because of the reduced repulsive interaction among Br_{ad} . The growth of a prewave at -1.1 V in KBr and CsBr [Fig. 1(a)] relates to the Br adsorption promoted by the complex formation between the AM cation and Br.

Br coverage is twice as high as Cs coverage at -1.0 V, indicating that Br is adsorbed at the hollow site around the Cs-Br complex already formed on the surface [Fig. 4(b)]. At the intermediate Br coverage, hydrated Cs contacts two or three Br adatoms, forming Cs- Br_2 and Cs- Br_3 complexes. Cs coverage reaches a first maximum at -1.0 V and then a local minimum at -0.8 V. The reduction of Cs coverage around -0.8 V is due to the release of excess Cs by Cs- Br_3 and Cs- Br_4 complexes

formation [Figs. 4(c) and 4(d)]. The increase in Br coverage narrows the areal space occupied by Cs on the surface, which expands the Ag-Cs layer spacing. Formation of the Cs-Br complex stabilizes the disordered Br layer and promotes the order-disorder transition of the Br layer. Finally, the coverage ratio of Br to Cs reaches to about four at -0.8 V with partial $c(2 \times 2)$ formation [Fig. 4(d)]. Above this potential, hydrated Cs is located at the hollow site of the $c(2 \times 2)$ -2Br layer.⁴

Heavy AM cation causes the negative shift of the potentials of the Br adsorption as well as the order-disorder transition. The order-disorder transition occurs at -0.82 V in 0.1 M CsBr, as shown in Fig. 1(a). This critical coverage of Br is $\theta_{\text{Br}} = 0.33$ (at -0.8 V), which is close to the values estimated by the simulation ($\theta_{\text{Br}} = 0.36$) and the SXD measurement ($\theta_{\text{Br}} = 0.25$) in 0.05 M NaBr.^{10,26,27} Ocko *et al.* concluded that the presence of water in the EDL does not affect the critical coverage of the order-disorder transition significantly compared with the theoretical and UHV results.¹⁰ Our results also support that cationic species does not affect the critical coverage, suggesting that interaction between Cs and Br in the complex is weak and noncovalent via hydration water. The promotive effect of Li on Br adlayer formation is smaller than those of K or Cs. However, it was reported that fuel cell reactions are inhibited by the strong interactions of Li and Na with OH_{ad} .⁵ Li and Na may have a particular affinity for oxygen species. Therefore, Cs and K with smaller hydration energy can strongly interact with Br_{ad} .

The anodic currents of the AgBr layer formation around 0 V also depends on the alkali metal cations. In CsBr, the onset potential of anodic current is shifted to negative potential [Fig. 1(a)]. The presence of Cs- Br_4 complex in the $c(2 \times 2)$ -2Br may promote the surface oxidation.

IV. SUMMARY

We determined the potential dependence of the coverage and the layer distance of ionic species in the electrical double layer by *in-situ* measurement of the x-ray specular rod. We revealed the promotive effect of AM cations on Br adsorption and the order-disorder transition on Ag(100). The x-ray specular rod shows that Cs approaches the surface at the initial stage of Br adsorption via noncovalent interaction. These results suggest that Br adsorption is promoted by the complex formation between the AM cation and Br_{ad} .

ACKNOWLEDGMENTS

X-ray measurements were supported by JASRI/SPring-8 under proposal numbers 2008B1395, 2009B1363, 2010B1070, and 2011A1119. This paper was supported by the Salt Science Research Foundation and Grant-in-Aid (KAKENHI) for Young Scientists (B) No. 22710099.

*mnakamura@faculty.chiba-u.jp

¹*Interfacial Electrochemistry*, edited by A. Wieckowski (Marcel Dekker, New York, 1999).

²O. M. Magnussen, *Chem. Rev.* **102**, 679 (2002).

³N. Garcia, V. Climent, J. M. Orts, J. M. Feliu, and A. Aldaz, *ChemPhysChem* **5**, 1221 (2004).

⁴M. Nakamura, N. Sato, N. Hoshi, and O. Sakata, *ChemPhysChem* **12**, 1430 (2011).

- ⁵D. Strmcnik, K. Kodama, D. Vliet, J. Greeley, V. R. Stamenkovic, and N. M. Markovic, *Nat. Chem.* **1**, 466 (2009).
- ⁶E. Sitta, B. C. Batista, and H. Varela, *Chem. Commun.* **47**, 3775 (2011).
- ⁷M. Nakamura and M. Ito, *Surf. Sci.* **490**, 301 (2001).
- ⁸M. Nakamura, Y. Shingaya, and M. Ito, *Surf. Sci.* **502-503**, 474 (2002).
- ⁹B. N. J. Persson, *Surf. Sci. Rep.* **15**, 1 (1992).
- ¹⁰B. M. Ocko, J. X. Wang, and T. Wandlowski, *Phys. Rev. Lett.* **79**, 1511 (1997).
- ¹¹M. T. M. Koper, *J. Electroanal. Chem.* **450**, 189 (1998).
- ¹²M. T. M. Koper, *Electrochim. Acta* **44**, 1207 (1998).
- ¹³S. J. Mitchell, G. Brown, and P. A. Rikvold, *J. Electroanal. Chem.* **493**, 68 (2000).
- ¹⁴I. A. Hamad, P. A. Rikvold, and G. Brown, *Surf. Sci.* **572**, L355 (2004).
- ¹⁵T. Wandlowski, J. X. Wang, and B. M. Ocko, *J. Electroanal. Chem.* **500**, 418 (2001).
- ¹⁶S. Wang and P. A. Rikvold, *Phys. Rev. B* **65**, 155406 (2002).
- ¹⁷S. J. Mitchell, S. Wang, and P. A. Rikvold, *Faraday discuss.* **121**, 53 (2002).
- ¹⁸M. Nakamura, N. Sato, N. Hoshi, and O. Sakata, *Langmuir* **26**, 4590 (2010).
- ¹⁹H. Keller, M. Saracino, H. M. T. Nguyen, and P. Broekmann, *Phys. Rev. B* **82**, 245425 (2010).
- ²⁰O. Sakata, Y. Furukawa, S. Goto, T. Mochizuki, T. Uruga, K. Takeshita, H. Ohashi, T. Ohta, T. Matsushita, S. Takahashi, H. Tajiri, T. Ishikawa, M. Nakamura, M. Ito, K. Sumitani, T. Takahashi, T. Shimura, A. Saito, and M. Takahashi, *Surf. Rev. Lett.* **10**, 543 (2003).
- ²¹E. Vlieg, *J. Appl. Crystallogr.* **33**, 401 (2000).
- ²²J. X. Wang, I. K. Robinson, B. M. Ocko, and R. R. Adzic, *J. Phys. Chem. B* **109**, 24 (2005).
- ²³M. Nakamura, H. Kato, N. Hoshi, K. Sumitani, and O. Sakata, *J. Phys. Chem. C* **111**, 977 (2007).
- ²⁴Y. Grunder, D. Kaminski, F. Golks, K. Krug, J. Stettner, O. M. Magnussen, A. Franke, J. Stremme, and E. Pehlke, *Phys. Rev. B* **81**, 174114 (2010).
- ²⁵H. Over, H. Bludau, M. Skottke-Klein, G. Ertl, W. Moritz, and C. T. Campbell, *Phys. Rev. B* **45**, 8638 (1992).
- ²⁶D. W. Wood and M. Goldfinch, *J. Phys. A* **13**, 2781 (1980).
- ²⁷W. Kinzel and M. Schick, *Phys. Rev. B* **24**, 324 (1981).